DE GRUYTER

Biomed. Eng.-Biomed. Tech. 2020; 65(1): 23–32

Mehdi Rajabioun, Ali Motie Nasrabadi*, Mohammad Bagher Shamsollahi and Robert Coben

Effective brain connectivity estimation between active brain regions in autism using the dual Kalman-based method

Abstract: Brain connectivity estimation is a useful method to study brain functions and diagnose neuroscience disorders. Effective connectivity is a subdivision of brain connectivity which discusses the causal relationship between different parts of the brain. In this study, a dual Kalman-based method is used for effective connectivity estimation. Because of connectivity changes in autism, the method is applied to autistic signals for effective connectivity estimation. For method validation, the dual Kalman based method is compared with other connectivity estimation methods by estimation error and the dual Kalman-based method gives acceptable results with less estimation errors. Then, connectivities between active brain regions of autistic and normal children in the resting state are estimated and compared. In this simulation, the brain is divided into eight regions and the connectivity between regions and within them is calculated. It can be concluded from the results that in the resting state condition the effective connectivity of active regions is decreased between regions and is increased within each region in autistic children. In another result, by averaging the connectivity between the extracted active sources of each region, the connectivity between the left and right of the central part is more than that in other regions and the connectivity in the occipital part is less than that in others.

Keywords: autism; dual Kalman filter; effective connectivity; multivariate autoregressive model; source localization methods.

---

*Corresponding author: Ali Motie Nasrabadi, Department of Biomedical Engineering, Faculty of Engineering, Shahed University, Tehran 3319118651, Iran, E-mail: nasrabadi@shahed.ac.ir
Mehdi Rajabioun: Science and Research Branch, Islamic Azad University, Tehran 1477893855, Iran
Mohammad Bagher Shamsollahi: Faculty of Electrical Engineering, Sharif University of Technology, Tehran 1136511155, Iran
Robert Coben: Neurorehabilitation and Neuropsychological Services, Massapequa Park, NY 11762, USA; and Integrated Neuroscience Services, Fayetteville, AR 28304, USA

Introduction

The brain is one of the most important and complicated parts of the human body. The dynamic functions of the brain are nonlinear such as their chaotic and synchronized manner and understanding its functions is essential [1] for brain function analysis. Studying brain function can be very valuable and useful for the diagnosis and analysis of neuroscience disorders (like autism). Studying brain connectivity is an important field of brain function realization [2] which is about the interactions between different regions [1, 3, 4]. Three different types of connectivity were introduced in previous related papers [1, 3–5]. Anatomical or structural connectivity discusses the physical and structural interactions between synapses and neural units [6, 7]. Temporal correlation and statistical dependency between brain regions is defined as functional connectivity which can be introduced in time or frequency domains [8, 9]. The connectivity or relation of one brain region to another part of the brain is called effective connectivity, which is defined as a causal relationship between activities of two regions. This type of connectivity describes the effect of one source on another source or the activity of each source is caused by activities of other sources [7, 9–11].

Effective connectivity is internally generating a phenomenon of brain region activity which can be estimated by electroencephalography (EEG) or functional magnetic resonance imaging (fMRI) information. Effective brain connectivity can be calculated using fMRI data and structural equation modeling method. In some other papers, effective connectivity was estimated by functional connectivity with fMRI data [12, 13]. But fMRI data has low time resolution. In this study, EEG signals are used because of its high temporal resolution. The methods for estimating this connectivity are divided into data-based and model-based methods. The data-based methods are based on the data [14]. Directed information is one of these methods which is used for linear and nonlinear causality estimation. Transfer entropy (TE), correlation integral (CI) and their derivations are other examples of these measures [2, 10, 15, 16]. The model-based methods for effective connectivity

estimation are based on fitting a model on signals and the connectivity is calculated by estimating model parameters. Granger causality (GC) is one of the model-based methods for connectivity estimation which is based on the supposition that each cause precedes its effects. The GC method is used especially in the absence of a priori data of brain abnormal patterns [1, 17–20]. The other method which needs a model for connectivity estimation is the dynamic causal model (DCM) which quantifies neural connectivity by assuming a bilinear state space model. This method is used for nonlinear relation estimation and by physiological model consideration of neuronal dynamics. In this method, various model parameters are optimized by considering certain prior knowledge [1, 21–23]. The multivariate autoregressive (MVAR) model is used in some papers for connectivity estimations. In these methods, an MVAR model is fitted to data for temporal dependency estimations and the model parameters can be calculated using different methods [24–26]. The Yule-Walker and the modified Yule-Walker methods are basic and traditional simple methods for MVAR model parameter calculations [27–29]. Levinson recursion, the Burg-type Nuttall-Strand method, the Vieira-Morf method and the Newton-Raphson gradient search method are some important and traditional methods in this field [30]. The Bayesian estimation method was used by Penny and Roberts for MVAR parameter estimation [31]. The ordinary extended Kalman filter is used to estimate the MVAR parameters [32]. Neumaier and Schneider proposed least square estimate and eigenmodes for MVAR estimation [33–35]. For connectivity validations, some connectivity measures and features are extracted from GC and linear MVAR models like directed transfer function (DTF), partial directed coherence (PDC), direct directed transfer function (dDTF) and so on which have been proposed in related papers. These measures are used in the frequency domain for direction and strength estimation of multiple coupled interactions.

The method which is used in this study is the dual Kalman-based method [36]. In this method, firstly a source localization method is applied to EEG data. Then the MVAR model with unknown parameters is fitted to extracted sources or active sources over time. For the calculation of unknown model parameters, the dual Kalman filter is used to estimate the model parameters from observations (in our work EEG signals). In this method, estimation of MVAR model parameters is used for effective connectivity calculation. The dual Kalman filter has been used in other works for connectivity calculations. Omidvarnia et al. used it for estimating EEG sensor connectivity in newborns. In the dual Kalman-based method, the algorithm is applied to the source space because of volume conduction effects on sensor spaces [37]. Studying source space is more accurate and valuable because of entering volume conductor and tissue conductance in equations. The dual Kalman-based method has two major advantages. The first one is the parallel estimation of state and parameters in the MVAR model. So during connectivity estimations, the source activities (states) are updated and dynamic source localization is done. Therefore, this method is more accurate than the static source localization methods. The second advantage is its independence to any predefined condition such as physiological or anatomical knowledge. In the dual Kalman-based method, active sources are localized by source localization methods [36].

Autism is one of the complicated, neurodevelopmental and heterogeneous disorders which is characterized by abnormal and restricted language, emotional and social communicational functions and their qualitative impairment in environmental behavior and inflexibility. Subjects with autism have many features in their social and communicational behaviors, of which inability to speak, less attention to their environment, weak emotional display and disability to show appropriate facial reaction are the most significant features of autistic children. From another view, the biological and functional basis of autism is not well understood and connectivity estimation of the brain in autistic children can be useful in this field. Autism disorder mostly begins in early childhood or adolescence and 58% of adults with autism have epilepsy or seizure experience during their life [38–41]. According to the reports from research for autism (Center for Diseases Control and Prevention; CDC 2009), the rate of autism is increasing. Blaxill reports that the rate of autism has increased from less than three in 10,000 children in 1970 to more than 30 per 10,000 in 1990 in the United States. According to the CDC report in 2012, it has risen to one out of 88 children (one per 54 in male children) [39, 42].

The relationship between autism and effective connectivity has been studied and analyzed in some papers. According to previous works, there is an abnormal connectivity pattern in the brain of autistic children in specific regions. Most of the related papers deliberated that the effective connectivity is increased in the local regions and is decreased in long distance in autism [43–48]. According to Wass et al., the connectivity is increased in frontal and short neural paths and is decreased in long distance and posterior to anterior or temporal regions [45]. According to Coben et al. there is more coherence in frontal regions and less coherence in the bilateral posterior temporal regions when comparing autistic subjects with normal children. In another paper by Coben et al. GC is used for effective

connectivity estimation from EEG signals. Their study is on the prefrontal cortex (PFC), anterior cingulate and bilateral inferior parietal regions and the results are underconnectivity between regions which are in long distance from each other [49]. The relation between autism and effective connectivity during the emotional processing task was studied by Wicker et al. with fMRI and structural equation modeling. The first result of this study was that the effect of amygdala (AMG) activation on the dorsomedial prefrontal cortex (DMPFC) is absent and the effect of DMPFC on the dorsolateral prefrontal cortex (dLPFC) is observed in autism. Secondly, the influence of dLPFC on the ventral part of the PFC and ventrolateral prefrontal cortex (vLPFC) on superior temporal sulcus (STS) is weak in autism. Thirdly, the strong influence of LPFC on the fusiform gyrus is observed in autism [50]. According to the study by Grezes et al., abnormal inter-regional cerebral effective connectivity is observed in viewing fearful gestures. In this work, the abnormality is observed in the right temporal parietal junction (TPJ), gyrus, AMG and middle parts of STS. According to Grezes et al.'s study, there is no difference in effective connectivity between occipital and AMG, STS and AMG, fusiform gyrus and AMG. On the other hand, there is a weaker connectivity of AMG on fusiform gyrus and primary motor cortex in autism during the emotional task [40]. Minshew and Williams discovered from EEG signals that in autism the frontal coherence is increased and anterior to posterior temporal coherence is reduced [51]. Wataru Sato et al. used dynamic causal modeling on fMRI data during the dynamic facial expression task to estimate regional brain activity and effective connectivity. According to their results, the activity of autistic children in visual parts of the brain like middle temporal gyrus (MTG), fusiform gyrus, AMG, medial PFC and inferior frontal gyrus (IFG) is reduced. The effective connectivity between primary visual cortex-MTG-IFG is weaker in autism in comparison with the control group during the dynamic emotional facial expression task [39]. According to Shih et al.'s study, the effective connectivity by structural equation model (SEM) on fMRI data in imitation showed a significant reduction in the connectivity between inferior partial lobe (IPL) on IFG and an increased connectivity in dLPFC on IFG is observed in the autistic group [41].

In this study, the dual Kalman-based method which is proposed in the previous study [36] is applied to autistic signals to estimate connectivity between active brain sources and the results are compared with the connectivity of normal children. In the dual Kalman-based method, firstly a source localization method is applied to EEG signals and active sources are extracted. Then, the MVAR model is fitted to active sources and the state space is

formed by adding the relation of EEG signals and active regions (by the leadfield matrix). So the dual Kalman model is applied to the model to estimate two unknown parameters (the source activation and the relation between them). In other words, in this method, the dual Kalman filter is used for estimating the relation between active sources and the connectivity is calculated from the estimated relationship. In [36], the method is applied to generated signals with known connectivity and the accuracy of the method is analyzed for different conditions. But in this paper, the method is applied to real autistic and control signals. As evident from the previous paragraph, in autism the connectivity is changed and the connectivity between brain regions of autistic and normal children is different. The dual Kalman filter method which is discussed in previous paragraphs has acceptable estimation because of the parallel estimation with source activation and it does not require any predefined information about source positions. Therefore, applying the dual Kalman-based method to autistic and normal EEG signals can help us to learn about autism disorder and the comparison between brain connectivity of them can assist us in finding out more details about autism.

An overview of the dual Kalman-based method and its structure is provided in the section "Materials and methods". The section "Simulations and method validations" discusses the two phases of simulation. The first phase is the estimation of model parameters with different methods and comparison of estimation error of the dual Kalman-based method estimated parameters with other methods. In the second phase of simulations, the connectivity of active sources in autistic and normal subjects is compared by calculating their dDTF. Lastly, the results of the simulation and the connectivity comparison between autistic and normal subjects are discussed in the section "Model implementation and results".

Materials and methods

In the dual Kalman-based method, this filter is used to estimate the causal relations between active brain sources from which effective connectivity can be calculated. So this method firstly needs a source localization method for extracting active brain sources during the time samples, and secondly, needs a model to fit active source on it for parameter estimation. Lastly, the method parameters are estimated with the dual Kalman filter from its observations (EEG signals). The flowchart and steps of the dual Kalman-based methods are shown in Figure 1.

In the first step, static or dynamic source localization is applied to EEG signals which are recorded from sensors and active brain regions are extracted from them. Source localization methods try
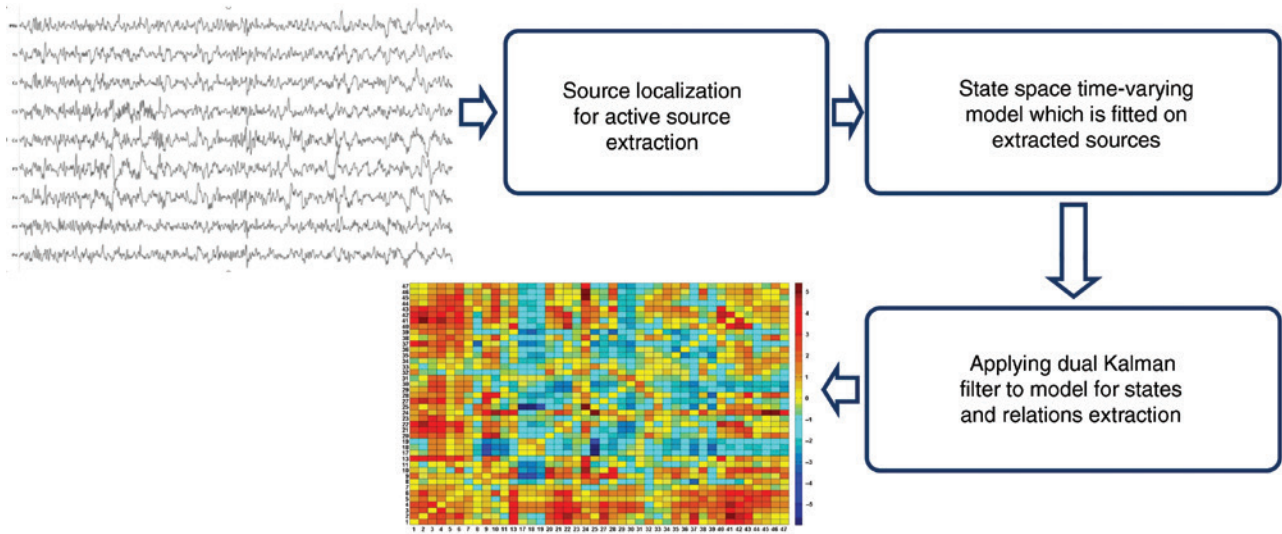
Figure 1: The steps of the dual Kalman-based method for connectivity estimation between active brain sources.
The method consists of three parts. Firstly, the source localization method is applied to EEG signals and active sources are extracted.
Then, the state space time-varying model is fitted to extracted active sources and lastly, the dual Kalman filter is applied to the model for estimating source activities and the relation between them.

to estimate the active source locations and activities using EEG signals which is called the EEG inverse problem. But before solving the inverse problem of EEG, EEG forward problem should be calculated using numerical finite element (FEM) or boundary element (BEM) methods and the relation between each source activation and EEG signals should be calculated (leadfield matrix calculation). The standard low resolution analysis (sLORETA) is one of the source localization methods which gives good and acceptable localization error in comparison with other methods [52, 53]. The explicit solution to this minimization problem in sLORETA is:

$$\widehat{J}_k = T \cdot V_k \tag{1}$$

where $\widehat{J}_k$ is the estimated source activation matrix, V_k is the EEG signal at sample k and T is defined as follows:

$$T = G^T H [H G G^T H + \alpha H]^+ \tag{2}$$

where G is the leadfield matrix, $[]^+$ is the pseudoinverse of matrix and in our method α is calculated using the Tikhonov regularization method and is set to 0.1 [54].

$$H = I - 11^T / 1^T 1 \tag{3}$$

The output of this part is the position of the limited number of active sources of the brain [52, 53].

The active sources which have bigger values in the estimated matrix are extracted during the time samples. For this purpose, the source localization method is applied to each sample of the EEG signal and the sources which are more active during the time are extracted as active sources and are used in the second subsection "Model implementation and results".

In the second part, the linear dynamic MVAR model is used for active sources modeling and the MVAR model is fitted to active sources which are extracted from the previous section. This model is defined as Eq. 4:

$$J_k = F_k J_{k-1} + \eta_k \tag{4}$$

where J_k is the kth sample of the source vector with $(n \times 1)$ and η_k is the state noise. In another equation, EEG signals are related to active sources by the leadfield matrix and can be written as Eq. 5:

$$V_k = G J_k + \varepsilon_k \tag{5}$$

where ε_k is the measurement noise at the kth sample.

So, the above two equations (Eq. 4 and Eq. 5) form a discrete linear state space equation.

$$\begin{aligned} J_{k+1} &= F_k J_k + \eta_k \\ V_k &= G J_k + \varepsilon_k \end{aligned} \tag{6}$$

where ε_k, η_k are the additive measurement and state noise, respectively. In Eq. 6, if both F_k and G are known, the extended Kalman filter is used for state estimation and J_k can be calculated from the observed EEG signal V_k. But if the relationship between states or F_k is unknown, J_k and F_k are calculated by the dual Kalman filter which can estimate both of them simultaneously with two parallel ordinary Kalman filters.

Generally, the dual Kalman filter is used for modeling, estimation and prediction tasks. In this paper and in the third part of the dual Kalman-based method, the modeling task is used and the parameters of the model are estimated from the signals or observations. In the dual Kalman method, states and model parameters are calculated from signals in parallel with each other.

Two ordinary Kalman filters are used in the dual Kalman filter for the simultaneous estimation of states and the relation between them. In the first Kalman filter, the model parameter $\widehat{F}_k$ is assumed to be known and the state vector is calculated, while another Kalman filter (called weight KF) is used for model parameter calculation by assuming that the current state $\widehat{J}_k$ is known. This process is done simultaneously and is schematically shown in Figure 2. So by estimating F by the dual Kalman filter, effective connectivity can be extracted. More details about this algorithm are explained in a previous paper [36].
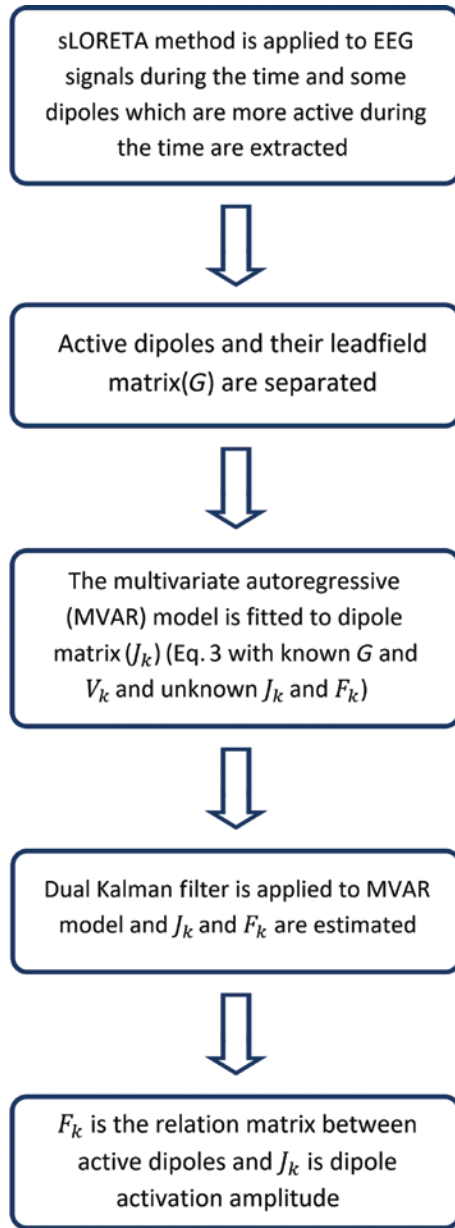
Figure 2: Parts of the dual Kalman filter.
The dual Kalman filter consists of two Kalman filters which work in parallel with each other. The above one is for state estimation and the bottom filter is for model parameter calculation.

Simulations and method validations

In this section, the method is applied to EEG signals which are recorded from autistic and control subjects. In the first phase of the simulation, the brain connectivity is estimated by several methods and EEG signals are calculated from estimated connectivities. Then estimation errors between calculated and real EEG signals are calculated. In the second phase of simulations, the relations between active sources are calculated by the dual Kalman-based method and dDTF as a measure of connectivity is calculated for autistic and normal signals. The calculated connectivities of both groups are compared with each other by dDTF measure.

The signals which are used in our simulations are recorded from HRL Laboratories and UCLA Semel Institute for Neuroscience and Human Behavior performed on autistic and control children. The signal recording device has a sampling frequency of 128 Hz and 19 recording channels with traditional 1020 standard electrode positions. The experimental group included 17 males and 10 females with age ranging from 4 to 12 years with a mean age of 6.1 years. The range and severity of autistic children are the same in the experimental test which is done by psychologists. The signals were recorded with eyes open and fixed on a spot directly in front of them. In this study, nine autistic and 18 control EEG signals are used for connectivity estimations.

In the preprocessing step after EEG acquisition, as a first step, for low frequency and baseline drift removal, a high-pass filter with a cut-off frequency of 1 Hz is applied to raw EEG. Then, independent component analysis (ICA) is applied to the filtered signals for independent component extraction. Lastly, the extracted components which are not based on brain activity (noise or artifacts) are removed. Some theories are used for detecting and rejecting the components which have noise or artifact [like electromyogram (EMG) or blinking artifact] [56–58]. Then, the resulting signals are normalized to the mean squares of them during the time.

In the first phase of simulation, the filtered signal is swept by a window with the known length (in this simulations it is 64 samples) and the model parameters of the sliding window are estimated using several methods (dual Kalman-based and other methods). Then, the value of the nth sample is estimated from p delayed samples of signal (n is the last sample of the sweeping window). In other methods which are used for MVAR model estimation, firstly the sensor space should be changed to a source space with leadfield matrix inversion and then the model parameters are estimated in the source space. After parameter estimation, the source activity is calculated from the estimated parameters and the estimated EEG signal in each sample is calculated from the source activity using Eq. 6. The estimation error is defined as the difference between the estimated and real EEG signals. In our simulation, the length of the window is set to 64 and the sweeping window is moved 32 samples in each run. In this part, p is calculated from Schwarz's Bayesian Criterion (BIC) model order of selection [59, 60]. After nth EEG sample calculations, the estimated sample is compared with a similar real data sample. For comparison, the mean square error between the estimated EEG signal and the real signal is defined as follows:

$$\mathrm{MSE}(n) = \frac{1}{L} \sum_{l=1}^{L} (\mathrm{EEG}_{\mathrm{estimated}}(n) - \mathrm{EEG}_{\mathrm{real}}(n))^2 \qquad (7)$$

where L is the number of EEG channels, n is the time sample, $\mathrm{EEG}_{\mathrm{estimated}}()$ is the estimated EEG signal in the nth sample which is calculated from the estimated model parameters and $\mathrm{EEG}_{\mathrm{real}}(n)$ is the real EEG value at the nth sample.

In the second phase of simulations, the dual Kalman-based method is applied to the filtered, preprocessed and normalized EEG signals of autistic and control subjects and the model parameters are estimated. Then dDTF measure of connectivity is calculated from the estimated parameters for comparing estimated connectivity between brain regions of autistic and normal subjects. Because of the different active regions in each signal, the brain is divided into eight regions. Then, the connectivity of active sources is calculated and the mean

value of sources connectivity in each region of the brain is calculated. The mean and standard deviation of estimated connectivity measures are calculated by applying the dual Kalman-based method to autistic and normal signals and the connectivity between eight brain subdivisions is calculated. The mean value of connectivity measures which are higher than the predefined threshold is selected to be shown in the α band. The α wave is a neural oscillation in 8–13 Hz which originates from the occipital lobe during wakeful relaxation with closed eyes. And DTF, PDC and dDTF are frequency-based measures and the brain waves (in this paper α) can be extracted from these measures.

For defining dDTF as a connectivity measure, the DTF should be defined as the causal influence of the brain cortical regions. This measure is introduced by supposing the process as MVAR as follows:

$$\sum_{k=0}^{p}\Lambda(k)Y(t-k)=E(t) \quad \text{with} \quad \Lambda(0)=I \tag{8}$$

where $Y(t)$ is a vector in time sample, $E(t)$ is a vector of uncorrelated white noise with zero-mean, $\Lambda(k)$ is the model parameter and p is the model order. Then, an MVAR model parameter is adequately estimated and it becomes the basis for subsequent spectral analysis. To investigate the spectral properties of the examined process, Eq. 8 is transformed to the frequency domain MVAR processes

$$\Lambda(f)Y(f)=E(f) \tag{9}$$

where

$$\Lambda(f)=\sum_{k=0}^{p}\Lambda(k)e^{-j2\pi f\Delta tk} \tag{10}$$

and Δt is the temporal interval between the two samples. Equation (9) can be written as

$$Y(f)=\Lambda^{-1}(f)E(f)=H(f)E(f) \tag{11}$$

$H(f)$ is the transfer matrix of the system, whose element H_{ij} represents the connection between the jth input and the ith output of the system.

The DTF coefficient is defined by

$$\theta_{ij}^{2}(f)=|H_{ij}(f)|^{2} \tag{12}$$

By normalizing the DTF coefficients for all elements, the other and main definition of DTF is:

$$\gamma_{ij}^{2}(f)=\frac{|H_{ij}(f)|^{2}}{\sum_{m=1}^{N}|H_{im}(f)|^{2}} \tag{13}$$

From the transfer matrix, we can calculate power spectra $S(f)$. If we denote by V the variance matrix of the noise $E(f)$, the power spectrum is defined by

$$S(f)=H(f)VH^{\star}(f) \tag{14}$$

where the superscript $\star$ denotes the transposition and complex conjugate. From $S(f)$, ordinary coherence can be computed as

$$k_{ij}^{2}(f)=\frac{|S_{ij}(f)|^{2}}{S_{ii}(f)S_{jj}(f)} \tag{15}$$

Coherence measures express the degree of synchrony (simultaneous activation) between areas i and j.

Partial coherence is another estimator of the relationship between a pair of signals, describing the interaction between areas i and j when the influence due to all $N-2$ time series is discounted (where N is the number of time series). It is defined by the formula

$$\chi_{ij}^{2}(f)=\frac{|M_{ij}(f)|^{2}}{M_{ii}(f)M_{jj}(f)} \tag{16}$$

where $M_{ij}(f)$ is the determinant of the minor matrix obtained by removing the ith row and jth column from the spectral matrix S.

DTF expresses direct and indirect connectivity between two signals and it is one of the disadvantages of DTF. So dDTF is introduced for direct connectivity expression. This criterion is defined by multiplying DTF by partial coherence.

$$\text{dDTF}=\chi_{ij}^{2}(f)k_{ij}^{2}(f) \tag{17}$$

where $k_{ij}^{2}(f)$ and $\chi_{ij}^{2}(f)$ are defined in Eqs. 13–17 [1, 61].

Model implementation and results

After simulations and EEG signal preprocessing and filtering, in this section, the dual Kalman-based method is applied to the filtered signal and some results are extracted. The steps of applying the dual Kalman-based method to signals for connectivity estimation are shown in Figure 3.

In the first phase which is defined in the "Simulations and method validations" section, EEG signals are preprocessed and filtered and the source localization method is applied to autistic and normal EEGs. After source localization, the MVAR model is fitted to active sources which are extracted, the connectivity estimation is done using several methods. For comparison, some traditional methods in MVAR parameter estimations are used. So, firstly the leadfield matrix which is calculated from the forward problem is inverted and then it is multiplied by the second part of Eq. 6 and the time series of source activities is calculated. Then, the traditional MVAR estimating methods are applied to the first part of Eq. 6 and the relation between sources is estimated. By using the estimated relationship between sources in each window, the future value of each source activity and EEG signal is calculated. After relation between sources is estimated, EEG signal is calculated from the estimated relations and the error between the estimated signals and real data is calculated. In this phase, the moving window with 64 sample lengths is swept along the signal and moves 32 samples in each run. Then, connectivity and model parameters are calculated in the window and signal value at nth samples (where n is the last sample of the sweeping window) is calculated from the estimated model parameters. The real EEG signal is compared with the estimated one during the signal.

The methods which are used for model parameter estimation and whose estimation results are compared with the dual Kalman-based method are as follows:
– Partial correlation estimation: Nuttall-Strand (biased correlation function) [62]
– Least squares [33]
– Least squares with eigenmodes [33]
– Correlation function estimation method [34, 35]

The mean and standard deviation of mean square error during the signal at the last sample of moving the window (nth sample) are
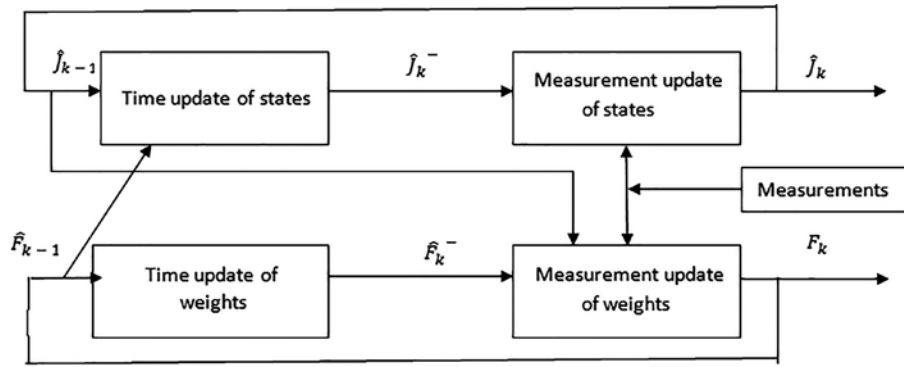
Figure 3: Flowchart and structure of the dual Kalman-based method.
In this method, firstly the sLORETA method is applied to EEG signals and active sources which are more active during the time are extracted. Then, the leadfield matrix and active sources are extracted. The MVAR method is fitted to the extracted sources and by adding the relation between sources and EEG signals the state space model is formed. In the state space model, the source activities during the time and their relations are unknown which are estimated with the dual Kalman filter.

shown in Table 1. In this simulation, nine autistic signals and 18 control signals from normal subjects are used and the mean and standard deviation of estimation errors are calculated.

As shown in Table 1, the dual Kalman-based method gives the least and the best estimation error in comparison with other methods and its result is more accurate than others in both autistic and normal signals.

In the second phase of simulations, the connectivity is estimated from autistic and normal EEG by the dual Kalman-based method. Then, dDTF measure is calculated from estimated connectivity and these measures are compared between autistic and normal subjects in α EEG band. In this simulation, the mean and standard deviation of these measures during all normal and autistic EEG signals are calculated between all brain subdivisions. The graphical plot of dDTF which is extracted from normal signal connectivity estimation is shown in Figure 4 and that from autistic signals is shown in Figure 5. In both plots, the standard divisions of dDTF is written in brackets ([]). It should be mentioned that, for clarification and the simple comparison between the two figures, the values of dDTF which are more than 0.1 are shown. The eight subdivisions of brains are abbreviated in figures as follows:

- Right frontal region (RF)
- Left frontal region (LF)
- Right central region (RC)
- Left central region (LC)
- Right partial region (RP)

- Left partial region (LP)
- Right occipital region (RO)
- Left occipital region (LO)

And for connectivity estimation between sources of each region, the connectivities between sources of the same region are estimated and the mean of them is calculated. For comparing and isolating between the two groups (autistic and control), the t-test algorithm is applied to both autistic and control classes and the p-value for each region is calculated and is shown in Table 2.

As evident from Figures 4 and 5, the connectivities between the left frontal region and central or partial regions are more than other region connectivities and are decreased in autism. This is in accordance with results of other papers in this field [43–46]. Also, the connectivities between the right and left part of the central and partial regions are decreased in autism. There are no active sources in some regions like the right frontal region. Other connectivities which have dDTF lower than 0.1 are not shown in the figures. By comparing dDTF of autistic and normal signals, it can be concluded that the dDTF between active sources in normal signals is more than that in autistic signals. In other words, by estimating the connectivity with the dual Kalman-based method and applying it to EEG signals, the connectivity between autistic brain regions is less than the normal connectivity. Another result which can be extracted from the table is the mean connectivity increment inside each region in autistic children.

Table 1: The mean and standard deviation of mean square error between the estimated and real signal at the last sample of the window over time.

	Method no. 1	Method no. 2	Method no. 3	Method no. 4	Dual Kalman-based method
Mean and standard deviation of autistic signals	0.0256±0.007576	0.0157±0.006584	0.0348±0.009445	0.1558±0.01698	0.0001587±0.00002544
Mean and standard deviation of normal signals	0.0171±0.00658	0.0115±0.00554	0.0258±0.00445	0.0965±0.00125	0.00009876±0.00001215

All methods are applied to signals and model parameters are estimated in each window. Then, the estimated EEG signal at the last sample of the window is calculated with model parameters. The calculated EEG value of the last sample of each window is compared with the real signal value by mean square error.
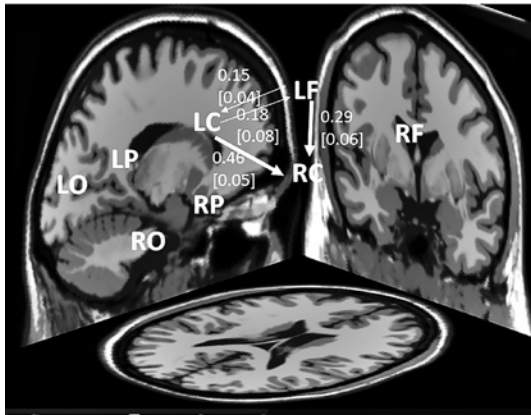
Figure 4: The mean and standard deviation (shown in brackets) of dDTF measures which are calculated from estimated connectivities by applying the dual Kalman-based method to 18 normal signals. The thickness of the arrows is related to its values. As shown, the connectivity between the central part of the brain (between the left and right side of the central part) is more than others (0.46 in our signals). In another result, the connectivity between the central parts and left frontal part of the brain is more than others.
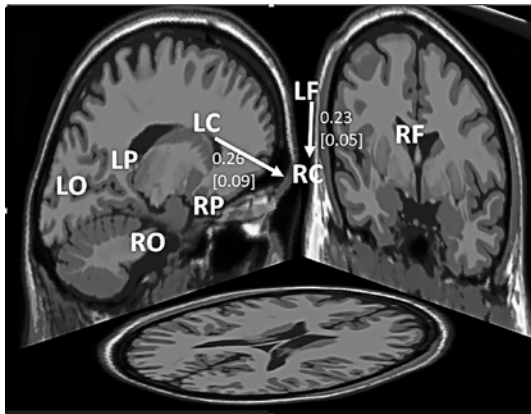

Figure 5: The mean and standard deviation (shown in brackets) of dDTF measures which are calculated from estimated connectivities by applying the dual Kalman-based method to nine autistic signals. The thickness of the arrows is related to its values. As shown, the connectivity between the left and right side of the central part of the brain is decreased in autism (0.26).

Discussion

Understanding dynamic functions of the brain and studying connectivity are important and useful subjects in diagnosing and analyzing several neurological disorders like autism. Effective brain connectivity is one of the connectivity divisions which discusses the causal relationship between the brain regions and interaction of one source or region with another. In this paper, the new dual

Table 2: The mean and standard deviation of estimated connectivity between sources which are in the same regions.

Mean and standard deviation of dDTF between each region	Control signals	Autistic signals	p-Value between two classes
RF	–	–	
LF	0.8252 ± 0.1164	0.9286 ± 0.0948	0.0075
RC	0.7672 ± 0.0752	0.8976 ± 0.1072	0.0001703
LC	0.6432 ± 0.1762	0.9352 ± 0.0851	0.000001735
RP	0.4523 ± 0.2071	0.6012 ± 0.0615	0.000093
LP	0.4782 ± 0.0982	0.5214 ± 0.1108	00236
RO	–	–	
LO	–	–	

The table shows the mean of connectivity inside each region.

Kalman-based method is applied to real signals for effective connectivity estimation. In the dual Kalman filter-based method, the source localization and connectivity estimation are calculated in parallel with each other and the connectivity is not calculated independently. So the connectivity estimation with this method is more accurate than the other methods in this field. Furthermore it does not need any predefined anatomical or physiological knowledge like the dynamic causal modeling methods. In the first simulation of this paper, the method ability in effective connectivity estimation is compared with other methods by estimation error. In this simulation, the connectivities between regions are extracted from the dual Kalman-based method and the signals are calculated from estimated connectivity. Then, the estimated error is calculated from the real and estimated signal difference. So the method which is used in this paper is more accurate and has less estimation error than other methods. As discussed already, because of parallel estimations of source or region connectivities and their activities, this method gives better results than other methods. Then, in the second phase of simulations, after method validation with estimation error, the effective connectivity is estimated from the EEG signals of autistic and control children. This study is done in the resting state and the connectivities between regions are estimated in this state (unlike other papers in which most of them are done in the stimulated state [38–45, 47]). And unlike other methods [38–45, 47] it does not need any anatomical information to target region localization. From the second simulation and by comparing effective connectivity between autistic and control children, the connectivities between active regions are decreased and the connectivities within regions are increased in accordance

with the results of other papers [38–48]. The regions of the left frontal lobe and central or partial regions have more connectivity measure value than other regions which is coincident with other papers in this field [43–46]. In another result, there are not any active sources in the right frontal region and the connectivities between the occipital region and other regions have less value than the threshold and it does not show in figures.

Author Statement

Research funding: This study was not funded and the authors declare that they have no conflict of interest.
Conflict of interest: Authors state no conflict of interest.
Informed consent: Informed consent was obtained from all individual participants included in the study.
Ethical approval: All procedures performed in studies involving human participants were in accordance with the ethical standards of the institutional and/or national research committee and with the 1964 Helsinki declaration and its later amendments or comparable ethical standards.

References

[1] Sakkalis V. Review of advanced techniques for the estimation of brain connectivity measured with EEG/MEG. Comput Biol Med 2011;41:1110–7.

[2] Friston KJ. Functional and effective connectivity in neuroimaging: a synthesis. Hum Brain Mapp 1994;2:56–78.

[3] Berry T, Hamilton F, Peixoto N, Sauer T. Detecting connectivity changes in neuronal networks. J Neurosci Methods 2012;209:388–97.

[4] Li Y, Tang X, Xu Z, Liu W, Li J. Temporal correlation between two channels EEG of bipolar lead in the head midline is associated with sleep-wake stages. Australas Phys Eng Sci Med 2016;39:147–55.

[5] Greenblatt RE, Pflieger ME, Ossadtchi AE. Connectivity measures applied to human brain electrophysiological data. J Neurosci Methods 2012;207:1–16.

[6] Billinger M, Brunner C, Müller-Putz GR. Online visualization of brain connectivity. J Neurosci Methods 2015;256:106–16.

[7] Sargolzaei S, Cabrerizo M, Goryawala M, Eddin AS, Adjouadi M. Scalp EEG brain functional connectivity networks in pediatric epilepsy. Comput Biol Med 2015;56:158–66.

[8] Ahmad RF, Malik AS, Kamel N, Reza F, Abdullah JM. Simultaneous EEG-fMRI for working memory of the human brain. Australas Phys Eng Sci Med 2016;39:363–78.

[9] Plis SM, Weisend MP, Damaraju E, Eichele T, Mayer A, Clark VP, et al. Effective connectivity analysis of fMRI and MEG data collected under identical paradigms. Comput Biol Med 2011;41:1156–65.

[10] Khadem A, Hossein-Zadeh G-A. Estimation of direct nonlinear effective connectivity using information theory and multilayer perceptron. J Neurosci Methods 2014;229:53–67.

[11] Vicente R, Wibral M, Lindner M, Pipa G. Transfer entropy – a model-free measure of effective connectivity for the neurosciences. J Comput Neurosci 2011;30:45–67.

[12] Robinson PA, Sarkar S, Pandejee GM, Henderson JA. Determination of effective brain connectivity from functional connectivity with application to resting state connectivities. Phys Rev E Stat Nonlin Soft Matter Phys 2014;90:012707.

[13] Mehta-Pandejee G, Robinson PA, Henderson JA, Aquino KM, Sarkar S. Inference of direct and multistep effective connectivities from functional connectivity of the brain and of relationships to cortical geometry. J Neurosci Methods 2017;283:42–54.

[14] Florin E, Pfeifer J. Statistical pitfalls in the comparison of multivariate causality measures for effective causality. Comput Biol Med 2013;43:131–4.

[15] Garcia-Zapirain B, Garcia-Chimeno Y, Saralegui I, Fernandez-Ruanova B, Martinez R. Differences in effective connectivity between children with dyslexia, monocular vision and typically developing readers: a DTI study. Biomed Signal Process Control 2016;23:19–27.

[16] Liu Y, Aviyente S. Quantification of effective connectivity in the brain using a measure of directed information. Comput Math Methods Med 2012;2012:16.

[17] Barnett L, Seth AK. The MVGC multivariate Granger causality toolbox: a new approach to Granger-causal inference. J Neurosci Methods 2014;223:50–68.

[18] Lenis G, Kircher M, Lázaro J, Bailón R, Gil E, Doessel O. Separating the effect of respiration on the heart rate variability using Granger's causality and linear filtering. Biomed Signal Process Control 2017;31:272–87.

[19] Tao C, Feng J. Nonlinear association criterion, nonlinear Granger causality and related issues with applications to neuroimage studies. J Neurosci Methods 2016;262:110–32.

[20] Sakkalis V, Giurcaneanu CD, Xanthopoulos P, Zervakis ME, Tsiaras V, Yang Y, et al. Assessment of linear and nonlinear synchronization measures for analyzing EEG in a mild epileptic paradigm. IEEE Trans Inf Technol Biomed 2009;13:433–41.

[21] Aponte EA, Raman S, Sengupta B, Penny WD, Stephan KE, Heinzle J. mpdcm: a toolbox for massively parallel dynamic causal modeling. J Neurosci Methods 2016;257:7–16.

[22] Nováková J, Hromčík M, Jech R. Dynamic causal modeling and subspace identification methods. Biomed Signal Process Control 2012;7:365–70.

[23] Pyka M, Heider D, Hauke S, Kircher T, Jansen A. Dynamic causal modeling with genetic algorithms. J Neurosci Methods 2011;194:402–6.

[24] Möller E, Schack B, Arnold M, Witte H. Instantaneous multivariate EEG coherence analysis by means of adaptive high-dimensional autoregressive models. J Neurosci Methods 2001;105:143–58.

[25] Erla S, Faes L, Nollo G, Arfeller C, Braun C, Papadelis C. Multivariate EEG spectral analysis evidences the functional link between motor and visual cortex during integrative sensorimotor tasks. Biomed Signal Process Control 2012;7:221–7.

[26] Motamedi-Fakhr S, Moshrefi-Torbati M, Hill M, Hill CM, White PR. Signal processing techniques applied to human sleep EEG signals – a review. Biomed Signal Process Control 2014;10:21–33.

[27] Aktaruzzaman M, Sassi R. Parametric estimation of sample entropy in heart rate variability analysis. Biomed Signal Process Control 2014;14:141–7.

[28] Mahmoudi A, Karimi M. Estimation of the parameters of multi-channel autoregressive signals from noisy observations. Signal Process 2008;88:2777–83.

[29] Wei Xing Z. Autoregressive parameter estimation from noisy data. IEEE Trans Circ Syst II: Analog Digit Signal Process 2000;47:71–5.

[30] Schlögl A. A comparison of multivariate autoregressive estimators. Signal Process 2006;86:2426–9.

[31] Penny WD, Roberts SJ, editors. Bayesian methods for autoregressive models. Neural Netw Signal Process, IEEE Signal Process Society Workshop, 2000.

[32] Milde T, Leistritz L, Astolfi L, Miltner WH, Weiss T, Babiloni F, et al. A new Kalman filter approach for the estimation of high-dimensional time-variant multivariate AR models and its application in analysis of laser-evoked brain potentials. NeuroImage 2010;50:960–9.

[33] Neumaier A, Schneider T. Estimation of parameters and eigen-modes of multivariate autoregressive models. ACM Trans Math Softw 2001;27:27–57.

[34] Guang-Te W, Singh VP. An autocorrelation function method for estimation of parameters of autoregressive models. Water Resour Manag 1994;8:33–55.

[35] Berndt H. Correlation function estimation by a polarity method using stochastic reference signals. IEEE Trans Inf Theory 1968;14:796–801.

[36] Rajabioun M, Nasrabadi AM, Shamsollahi MB. Estimation of effective brain connectivity with dual Kalman filter and EEG source localization methods. Australas Phys Eng Sci Med 2017;40:675–86.

[37] Omidvarnia AH, Mesbah M, Khlif MS, O'Toole JM, Colditz PB, Boashash B. Kalman filter-based time-varying cortical connectivity analysis of newborn EEG. Conf Proc IEEE Eng Med Biol Soc 2011;2011:1423–6.

[38] Jack A, Morris JP. Neocerebellar contributions to social perception in adolescents with autism spectrum disorder. Dev Cogn Neurosci 2014;10:77–92.

[39] Sato W, Toichi M, Uono S, Kochiyama T. Impaired social brain network for processing dynamic facial expressions in autism spectrum disorders. BMC Neurosci 2012;13:99.

[40] Grezes J, Wicker B, Berthoz S, de Gelder B. A failure to grasp the affective meaning of actions in autism spectrum disorder subjects. Neuropsychologia 2009;47:1816–25.

[41] Shih P, Shen M, Ottl B, Keehn B, Gaffrey MS, Muller RA. Atypical network connectivity for imitation in autism spectrum disorder. Neuropsychologia 2010;48:2931–9.

[42] Belmonte MK, Allen G, Beckel-Mitchener A, Boulanger LM, Carper RA, Webb SJ. Autism and abnormal development of brain connectivity. J Neurosci 2004;24:9228.

[43] Cornew L, Roberts TP, Blaskey L, Edgar JC. Resting-state oscillatory activity in autism spectrum disorders. J Autism Dev Disord 2012;42:1884–94.

[44] Isler JR, Martien KM, Grieve PG, Stark RI, Herbert MR. Reduced functional connectivity in visual evoked potentials in children with autism spectrum disorder. Clin Neurophysiol 2010;121:2035–43.

[45] Wass S. Distortions and disconnections: disrupted brain connectivity in autism. Brain Cognit 2011;75:18–28.

[46] Vissers ME, Cohen MX, Geurts HM. Brain connectivity and high functioning autism: a promising path of research that needs refined models, methodological convergence, and stronger behavioral links. Neurosci Biobehav Rev 2012;36:604–25.

[47] Barttfeld P, Wicker B, Cukier S, Navarta S, Lew S, Leiguarda R, et al. State-dependent changes of connectivity patterns and functional brain network topology in autism spectrum disorder. Neuropsychologia 2012;50:3653–62.

[48] Uddin LQ, Supekar K, Menon V. Reconceptualizing functional brain connectivity in autism from a developmental perspective. Front Hum Neurosci 2013;7:458.

[49] Coben R, Mohammad-Rezazadeh I, Cannon RL. Using quantitative and analytic EEG methods in the understanding of connectivity in autism spectrum disorders: a theory of mixed over- and under-connectivity. Front Hum Neurosci 2014;8:45.

[50] Wicker B, Fonlupt P, Hubert B, Tardif C, Gepner B, Deruelle C. Abnormal cerebral effective connectivity during explicit emotional processing in adults with autism spectrum disorder. Soc Cogn Affect Neurosci 2008;3:135–43.

[51] Minshew NJ, Williams DL. The new neurobiology of autism: cortex, connectivity, and neuronal organization. Arch Neurol 2007;64:945–50.

[52] Grech R, Cassar T, Muscat J, Camilleri KP, Fabri SG, Zervakis M, et al. Review on solving the inverse problem in EEG source analysis. J Neuroeng Rehabil 2008;5:25.

[53] Jatoi MA, Kamel N, Malik AS, Faye I. EEG based brain source localization comparison of sLORETA and eLORETA. Australas Phys Eng Sci Med 2014;37:713–21.

[54] Calvetti D, Morigi S, Reichel L, Sgallari F. Tikhonov regularization and the L-curve for large discrete ill-posed problems. J Comput Appl Math 2000;123:423–46.

[55] Kuhlman WN. Functional topography of the human mu rhythm. Electroencephalogr Clin Neurophysiol 1978;44:83–93.

[56] Emily SK, Steven JL, Scott M, Julie O. ERP Features and EEG Dynamics an ICA Perspective. Oxford University Press. https://sccn.ucsd.edu/~scott/pdf/Makeig_Onton_LuckERP11.pdf.

[57] Onton J, Makeig S. Information-based modeling of event-related brain dynamics. Prog Brain Res 2006;159:99–120.

[58] Delorme A, Makeig S. EEGLAB: an open source toolbox for analysis of single-trial EEG dynamics including independent component analysis. J Neurosci Methods 2004;134:9–21.

[59] Sugiyama M, Ogawa H. Theoretical and experimental evaluation of the subspace information criterion. Mach Learn 2002;48:25–50.

[60] Draper NR, Guttman I. A Common Model Selection Criterion. Probability and Bayesian Statistics. Boston, MA, USA: Springer US; 1987:139–50.

[61] Melia U, Vallverdu M. Methods in Brain Connectivity. Inference Through Multivariate Time Series Analysis. Koichi Sameshima, Luiz Antonio Baccalá. Front Neuroeng. Boca Raton, FL, USA: CRC Press, Taylor & Francis Group; 2014.

[62] Rodrigues PL, Baccala LA. A new algorithm for neural connectivity estimation of EEG event related potentials. Conf Proc IEEE Eng Med Biol Soc 2015;2015:3787–90.